

SIXTH EUROPEAN ROTORCRAFT AND POWERED LIFT AIRCRAFT FORUM

Paper No. 49

ADVANCED RESEARCH ON HELICOPTER BLADE AIRFOILS

J.J. Thibert

ONERA

J. Gallot

AÉROSPATIALE

France

Septembre 16-19, 1980

Bristol, England

THE UNIVERSITY, BRISTOL, BS8 1 HR, ENGLAND

ADVANCED RESEARCH ON HELICOPTER BLADE AIRFOILS

by Jean-Jacques THIBERT

Office National d'Etudes et de Recherches Aéronautiques (ONERA)
92320 Châtillon (France)

and Jacques GALLOT

Société Nationale Industrielle Aéronautique
13722 Marignane (France)

ABSTRACT

ONERA and AEROSPATIALE have undertaken a joint programme for defining advanced airfoils for helicopter rotor blades. Three airfoils with a thickness to chord ratio of 7%, 9% and 12% respectively have been defined to specifications suited to the position of the airfoil along the blade span. The characteristics and performance data determined from wind-tunnel testing are presented and compared with those of other known airfoils and with the figures expected from computation methods.

Construction of model rotors has been decided for testing this new generation of airfoils; experiments carried out in S1 wind tunnel in Modane allowed confirming the expected gains. These tests were complemented by in-flight testing of a set of blades with the OA209 airfoil on Dauphin helicopter. The complete set of results has guided the optimization of blades intended for use on Dauphin or Ecureuil series.

I - INTRODUCTION

With a view to improving the cost-effectiveness and the performance of their helicopters, AEROSPATIALE have entered upon a long-term research programme intended to increase the efficiency of the rotors in hover and forward flight as well (ref. 1). These researches were intended both to gain a deeper knowledge about rotor operational conditions (ref. 2 and 3) and to improve the airfoil or rotor performance prediction methods; experiments on model and full scale rotors as well made it possible to validate the theoretical researches.

Substantial improvements had already been obtained on the PUMA through the replacement of metal rotor blades by composite rotor blades; such improvements were due to the use of a higher twist and cambered profiles distributed over a spanwise evolutive blade. In 1974, in order to sustain such an effort, AEROSPATIALE, jointly with ONERA, initiated the development of a new family of profiles designed for replacing that used on the PUMA.

The first part of this paper specifies how the various profiles have been designed and gives a rough estimate of the results obtained both through calculation and tests. The second part details the experiment on model rotors which allowed to test this new generation of profiles and gives the first results obtained on a full scale rotor.

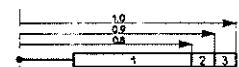
II DESIGN AND PERFORMANCES OF THE AIRFOIL FAMILY

2.1 - Design objectives

It is known that the helicopter blade profiles have to work in an extremely complicated flow environment. At the present time the airfoil design methods are unable to take into account the real nature of the flow field, particularly its unsteadiness. So the airfoils performances require-

ments are given in terms of steady values and deduced from the inspection in a (CL, M) plane of the operating conditions of the blade profile during a cycle for the three main flight areas: forward flight, hover and manoeuvres. The values of the design objectives depend on the helicopter mission and on the position of the airfoil along the blade span.

Fig. 1 shows the design objectives which have been settled for the study of the new blade rotor. The priorities for this new blade, which are the improvement of the performances in hover and forward flight, appear in this figure in the MDD and L/D constraints for all the sections. The C_{m0} constraints are also extremely severe even for the section 1 near the hub because for flexible blades, the torsion effect induced by a high C_{m0} would be prejudicial for the life duration of the control rods. A trailing edge tab has also been included in the airfoil definition in order to facilitate the manufacture of the blade.



FLIGHT CONDITIONS	PREPONDERANT AERODYNAMIC COEFFICIENT	SECTIONS		
		1	2	3
ADVANCING FLIGHT	Med of CL_{-0}	≥ 0.8	0.85	0.9
	$ C_{m0} $	≤ 0.01	0.01	0.01
HOVERING	L/D ratio at $M_0 = 0.5 - 0.6$ $CL = 0.8$	75	80	85
MANEUVER	$M = 0.3$	≥ 1.5	1.4	
	CL_{max}	≥ 0.6	1.3	1
	$M = 0.5$	≥ 1.3		
GEOMETRICAL CONSTRAINT	t/c	-12%	9%	-7%

Fig. 1 Requirements for a helicopter blade

The first airfoil designed for the section 2 of this new blade has been called OA209. Its design method and total performances deduced from wind tunnel tests have been presented in ref. 4. Fig. 2 from ref. 4 shows the performances of the OA209 airfoil in term of CL max, Mach drag divergence MDD, and zero lift pitching moment C_{m0} . In order to avoid any technological problem for manufacturing the blade the airfoils for the section 1 called OA212 and for the section 3 called OA207 have been derived geometrically from the basic airfoil OA209.

2.2 - Design and performances of the OA207 airfoil

The good performances in CL max of the basic airfoil of the family at low mach number is due to the shape of its leading edge and especially to the curvature evolution in that region; so the geometry of this airfoil has been kept both for the upper and lower surfaces up to the points of maximum thickness for the design of the OA207 airfoil. The aft part of the airfoil has been modified with an affinity parallel to the chord axis to obtain a chord length of 1.3.

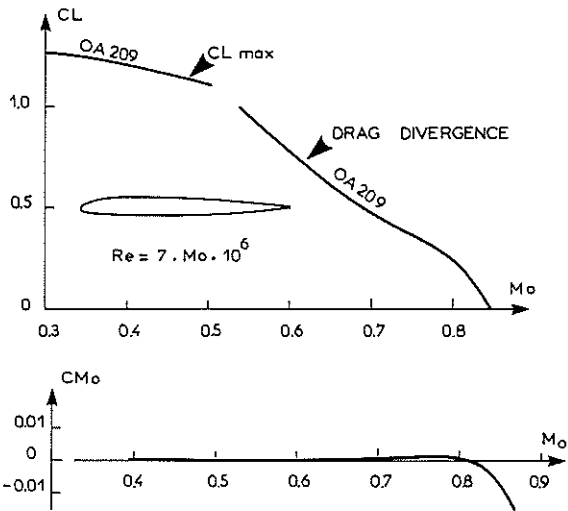


Fig. 2 OA209, Airfoil - Total performances

The contour of the airfoil OA207 designed by this method is shown fig. 3. Its thickness to chord ratio is 0.07.

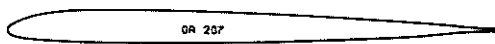


Fig. 3 OA207, Airfoil contour

The evaluation of the performances of this airfoil has been made with the transonic viscous code ref. 5. This code solves the full potential equation and the viscous effects are taking into account by adding the displacement thickness of the boundary layer on the airfoil contour.

This code has been calibrated with the tests results of various airfoils in the S3 Modane wind tunnel. These comparisons have shown that the prevision of the drag coefficient and of the Mach drag divergence MDD are correct. However this code cannot predict the CL max because it is unable to compute configuration with boundary layer separation. So it is necessary to define empirical stall criteria concerning the main parameters governing the stall of an airfoil which are the maximum velocity on the upper surface leading edge and the recompression law following the expansion. The numerous tests made by ONERA in the S3 Ma wind tunnel show that it is possible to make a correlation between the value of the minimum pressure coefficient K_p at the stall and the thickness ratio for airfoils having low C_{mo} (i.e. the same class of velocity distribution along the chord), for a given Mach number and Reynolds number. The top of fig. 4 shows this correlation for $Mo = 0.4$ and $Re = 2.2 \cdot 10^6$ based on the chord. The change in the evolution of the minimum of K_p with t/c is due to the type of stall, generally leading edge stall for $t/c < 9\%$ and trailing edge stall for $t/c \geq 9\%$. For an airfoil with $t/c = 0.07$ the minimum value of K_p at the stall is -5.6 for this Reynolds number.

The evolution of the minimum of K_p computed with the transonic viscous code ref. 5 is shown at the bottom of fig. 4. However for thin airfoils the experimental minimum of pressure which is very close to the leading edge is not well defined due to the lack of pressure holes in this region, so the theory which is more precise in that region gives for the same level of lift a higher expansion. This discrepancy between theory and experiment has been calibrated with models having the same chord and the same equipment and has been estimated at $\Delta K_p = +0.4$.

This method gives an estimation of the CL max of the OA207 airfoil of 1.07.

The OA207 airfoil has been tested in two dimensional flow in the S3Ma wind tunnel (test section 0,56 m x 0,78 m) with a 0.21 m chord model at a Reynolds number related to the chord of $5 \times Mo \times 10^6$.

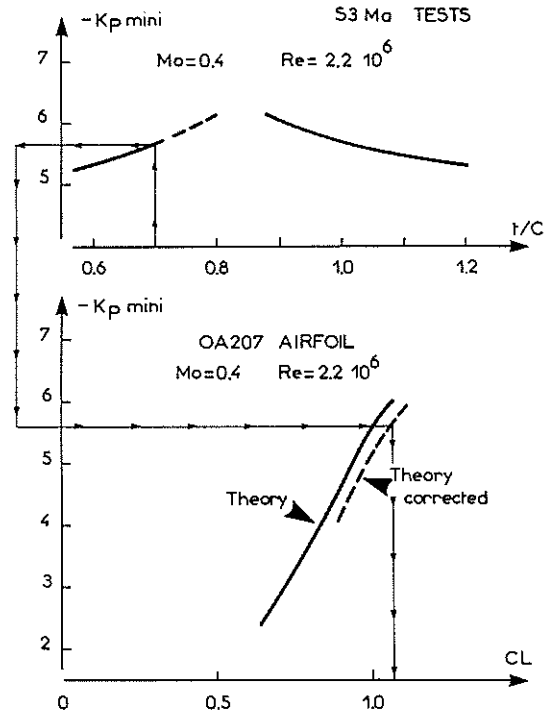


Fig. 4 OA207, Estimation of the CL max at $Mo=0.4$

The total performances of this airfoil are given in fig. 5 in a (CL, Mo) diagram. For Mach numbers $< 0,6$ the CL max has been drawn, and for Mach numbers $\geq 0,6$ the Mach drag divergence MDD at constant level of CL is given.

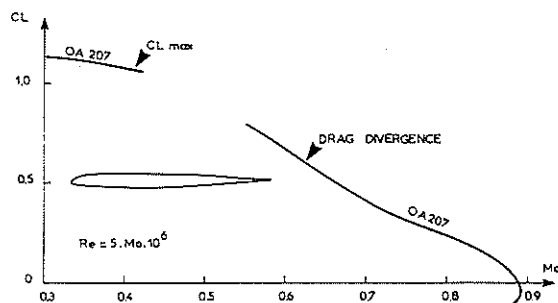


Fig. 5 OA207, Total performances

This airfoil has, in spite of its small thickness, quite a high level of CL max at low Mach numbers, since the CL max at $Mo = 0,3$ is 1.14 and 1.1 at $Mo = 0,4$, values higher than those obtained in the same wind tunnel on the NACA 0012 airfoil at the same Reynolds number. (CL max = 1. for the NACA 0012 at $Mo = 0,4$). So the estimated CL max at $Mo = 0.4$ is close to the experimental value.

The drag divergence Mach number of the OA207 airfoil is 0,895 for zero lift coefficient which is an increase of $\Delta M = 0.045$ compared to the basic airfoil OA209 and very close to the design objective of fig. 1.

Fig. 6 shows the evolution of the zero lift pitching moment coefficient C_{mo} versus mach num-

ber. The C_{mo} is slightly positive ($< 0,01$) up to the MDD, and beyond it becomes negative. The lift to drag ratio is 71 at $M_0 = 0,6$ and $CL = 0,6$ so slightly lower than the objective of fig. 1 but close to the value obtained with the OA209 airfoil which was 75.

Fig. 7 compares the OA207 performances to those of airfoils having about the same thickness ratio whose test results have been published. The comparisons are made in term of CL_{max} at $M_0 = 0,4$, MDD at $CL \sim 0$, C_{mo} at low mach numbers and CD at $M_0 = 0,6$ $CL = 0,6$. These airfoils are :

- NACA 0006
- Boeing Vertol airfoils V13006-0,7 and VR8
- Aérospatiale SA 13106-0,7



Fig. 6 OA207, Zero lift pitching moment coefficient

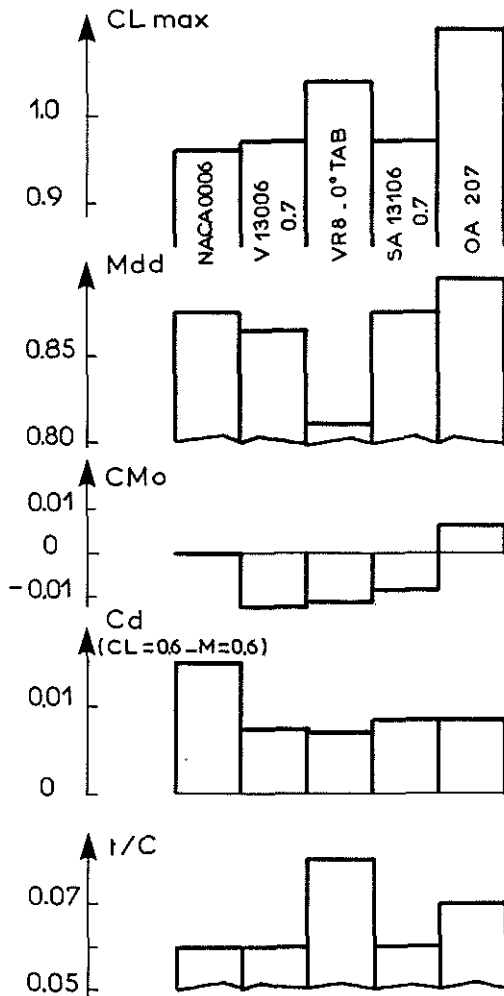


Fig. 7 OA207, Comparison with other airfoils

Performances of the NACA 0006 and Boeing Vertol airfoils have been found ref. 6 while the SA 13106 airfoil have been tested in the same conditions as the OA207 in the S3 Ma wind tunnel.

The OA207 airfoil has a higher CL_{max} than the other airfoils and in spite of its thickness ratio of 0,07, its MDD at $CL = 0$ is also higher than those of the airfoils of $t/c = 0,06$. Its CD at $M_0 = 0,6$ and $CL = 0,6$ is the same as for the SA 13106-0,7 and slightly higher than for the Boeing Vertol airfoils.

This thin airfoil has high performances in all the flight areas and gives substantial gains for high mach numbers compared to the OA209 airfoil so the tapering of the blade tip should increase the performances in high speed forward flight.

2.3 - Design and performances of the OA212 airfoil

For sections between 0 and 0.7 R along the span the main objectives are :

- high level of CL_{max} for $M_0 = 0,3$ to 0.5 to avoid stall on the retreating blade
- high L/D at $M_0 = 0,5 - 0,6$ and $CL = 0,6$ to reduce the power absorbed by rotor in hovering flight.

These objectives have to be reached without a great penalty in MDD performances compared to the airfoils of section 2 along the span (0.8 - 0.9R). The OA209 airfoil has a high MDD at $CL = 0$ due to its thickness distribution. So for design of the airfoil for inboard section 1 this thickness distribution has been transformed by affinity in order to obtain a 12 per cent thick airfoil. The camber distribution has been designed to reach the objectives of fig. 1 in CL_{max} at $M_0 = 0,3$ and $M_0 = 0,5$ without too high a nose down pitching moment coefficient C_{mo} . The OA212 airfoil obtained by this method is shown fig. 8.



Fig. 8 OA212, Airfoil contour

The CL_{max} of this airfoil at $M_0 = 0,3$ and $M_0 = 0,5$ have been evaluated using the same method as for the OA207. On the top of fig. 9 are shown the experimental evolutions of the minimum of K_p at the stall, deduced from the S3 Ma tests on airfoils with low C_{mo} , versus the thickness to chord ratio. For $M_0 = 0,3$ the curve has the same shape as for $M_0 = 0,4$ (fig. 4) with a change in the K_p evolution between 7 and 9 per cent due to the change of the type of stall.

At $M_0 = 0,5$ the evolution of K_p is very small because for this mach number the stall is due to the presence of a shock wave after the leading edge expansion which causes the separation of the boundary layer. For a 12 per cent thick airfoil the stall occurs when the K_p reaches the value of -6,6 at $M_0 = 0,3$ and -3,8 at $M_0 = 0,5$. The theoretical evolutions of the K_p mini for the OA212 airfoil are plotted on the bottom of fig. 9 for $M_0 = 0,3$ and $M_0 = 0,5$. Using the previous criteria the estimated CL_{max} are 1.56 at $M_0 = 0,3$ and 1.4 at $M_0 = 0,5$. However these values have to be reduced by 0,07 to take into account the discrepancies between theory and experiment, which appear for the pressure distribution near the trailing edge when the separation of the boundary layer occurs.

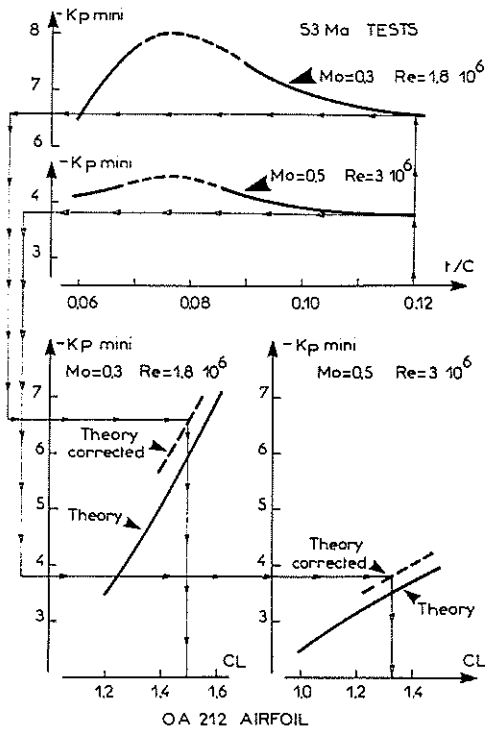


Fig. 9 OA212. Estimation of the CL max at $M_0 = 0.3$ and $M_0 = 0.5$

This value of $\Delta C_L = 0.07$ has been deduced from the calibration of the viscous code with experimental tests results. So the evaluations of CL max for the OA212 airfoil are 1.49 at $M_0 = 0.3$ and 1.33 at $M_0 = 0.5$.

The experimental tests results of this airfoil obtained in the S3 Ma wind tunnel on a 0.210 m model are plotted in fig. 10. The CL max is 1.43 at $M_0 = 0.3$ and 1.33 at $M_0 = 0.5$.

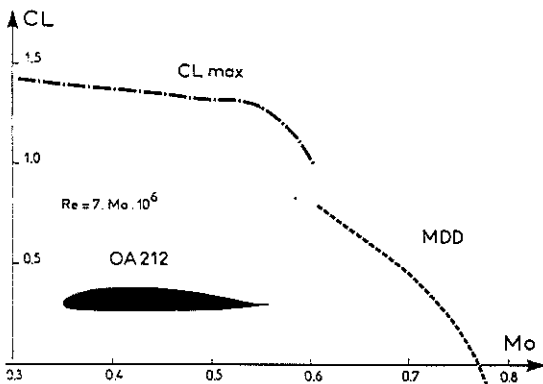


Fig. 10 OA212. Total performances

For $M_0 = 0.3$ the C_L max is slightly lower than the evaluation due to the trailing edge separation which is shown by the evolution of the trailing edge pressure fig. 11. Tests at a higher Reynolds number have given a C_L max of 1.47 at $M_0 = 0.3$. The other performances of this airfoil are :

- MDD = 0.77 at CL = 0
- L/D = 67 at $M_0 = 0.6$ CL = 0.6
- $C_{mo} = -0.002$ at Mach number = 0.4

In fig. 12 these performances are compared with those of other airfoils having the same thickness to chord ratio.

These airfoils are :

- NACA profiles NACA 0012 NACA 63A012
- profiles deduced from NACA series

ONERA "NACA cambré" Aérospatiale SA 13112 - Boeing Vertol V43012-1.58 - VR7.

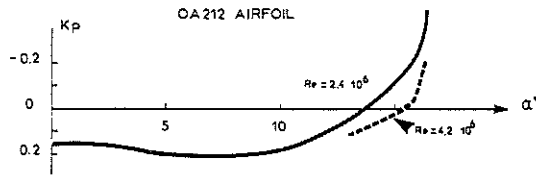


Fig. 11 OA212. Reynolds number effect at $M_0 = 0.3$

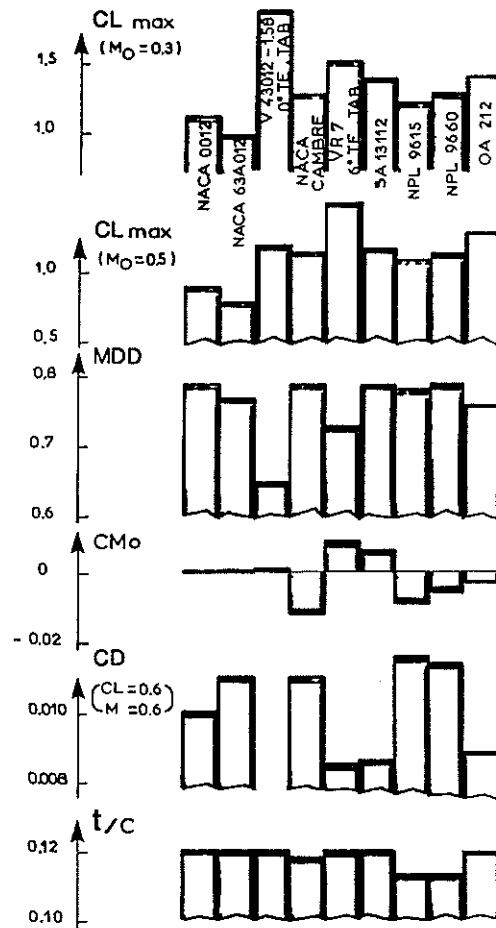


Fig. 12 OA212. Comparison with other airfoils

The NACA 0012, "NACA cambré" and SA13112 airfoils have been tested in the S3Ma wind tunnel at the same Reynolds number as the OA212 airfoil. The test results for the other airfoils have been found ref. 6 and ref. 7 .

- The symmetrical NACA airfoils have poor maximum lift capability while the V43012-1.58 has a very high CL max at $M_0 = 0.3$ but its performances decrease rapidly with mach number and its MDD is 0.65.

- The ONERA "NACA cambré" has not very high CL max and its drag coefficient is also high at $M_0 = 0.6$ CL = 0.6

- The NPL airfoils have high MDD but their performances are not good in CL max and poor in

CD at $M_0 = 0.6$

- The VR7 has good performances in CL max especially at $M_0 = 0.5$ and a low CD at $M_0 = 0.6$ CL = 0.6 but its MDD is not very high.

- The SA 13112 has overall good performances but the OA212 airfoil has better CL max at $M_0 = 0.5$ and higher L/D for high levels of CL at $M_0 = 0.5$ and 0.6.

Fig. 13 shows the C_m evolution with lift at $M_0 = 0.3$ for the VR7 without and with -6° tab deflection and for the OA212 airfoils. Though the tab deflection on the VR7 gives substantial improvement, the value of C_m for this airfoil remains very high for high lift level while for the OA212 the C_m value does not exceed -0.01 . This good behaviour at high lift is very valuable and this airfoil should not give blade torsion in hover and maneuver flight which induces pitch link loads and might be prejudicial for the life duration of the control rods and the vibratory level.

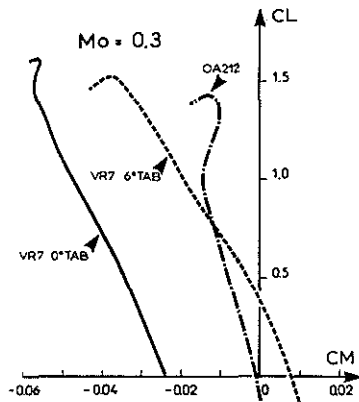


Fig. 13 - C_m evolution with C_L at $M_0 = 0.3$

2.4 - Summary of the airfoil family performances

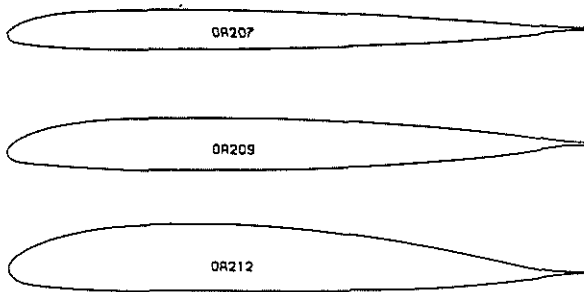


Fig. 14 Contours of the OA family of airfoils

The contours of the three airfoils OA212 OA209 and OA207 are drawn fig. 14. A complete review of their performances is given fig. 15 in a form suggested ref. 6. On figs. 16, 17 and 18 are plotted the main total performances of the three airfoils compared to those of the NACA 0012 to show the improvements which can be obtained on a tapered blade equipped with modern airfoils. The main total performances are :

- CL max for $M_0 = 0.5$ and MDD at constant

CL for $M_0 = 0.5$ fig. 16

- Drag polars at $M_0 = 0.5$ and 0.6 fig. 17

- Evolutions of the CD at CL = 0.1 with Mach number fig. 18.

No.	OBJECTIVE	TEST DATA		
		OA 207	OA 209	OA 212
1	C_{mo} at $M = 0.3$.0046	0.002	-0.0013
2	C_{LMAX} at $M = 0.4$	1.1	1.21	1.37
3	MDD_0	0.695	0.85	0.77
4	C_{mo} at $M = 0.7$.007	0	-0.01
5	C_d for $C_L = .6$ and $M = .6$.0084	.008	.0090
6	C_{LMAX} at $M = 0.5$	0.97	1.12	1.33
7	C_m at $C_L = 1.0$ and $M = 0.3$	-	0.	-0.014
8	C_{d_0} at $M = MDD_0 + 0.02$.017	.0165	.016
9	M_T at $C_L = 0$	0.88	0.85	0.785
10	$M^2 C_{mo}$ at MDD_0	0	-.004	-0.01
11	Type of Stall at $M = 0.3$ and $M = 0.4$	L.E	T.E	T.E
		L.E	T.E	T.E
12	C_{d_0} at $MDD_0 - 0.1$.0081	.0084	.0087

Fig. 15 OA airfoil family. Complete review of the performance

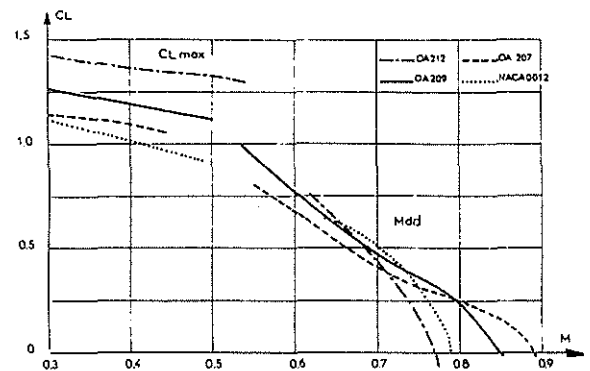


Fig. 16 Total performance of the OA airfoils

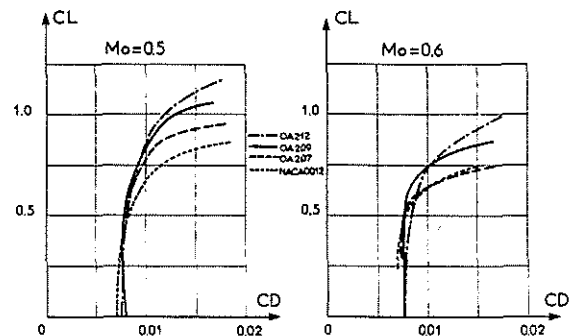


Fig. 17 Drag polar of the OA airfoils

Compared to the NACA 0012 airfoil the gains are important in CL max and L/D for $C_L > 0.5$. The improvement in MDD given by the thinner airfoils are of course spectacular but it should be outlined

that the level of CD at low mach number on the new airfoils are greater than on the NACA 0012.

This is due to the fact that on these cambered airfoils the transition of the boundary layer on the lower surface is due to the compression following the leading edge suction peak while on the NACA 0012, for the test Reynolds number, transition occurs at the shock.

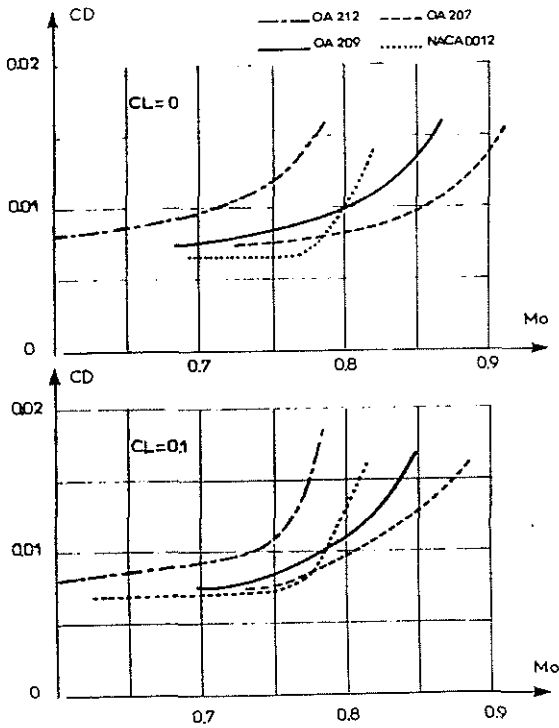


Fig. 18 Drag evolution of the OA airfoils

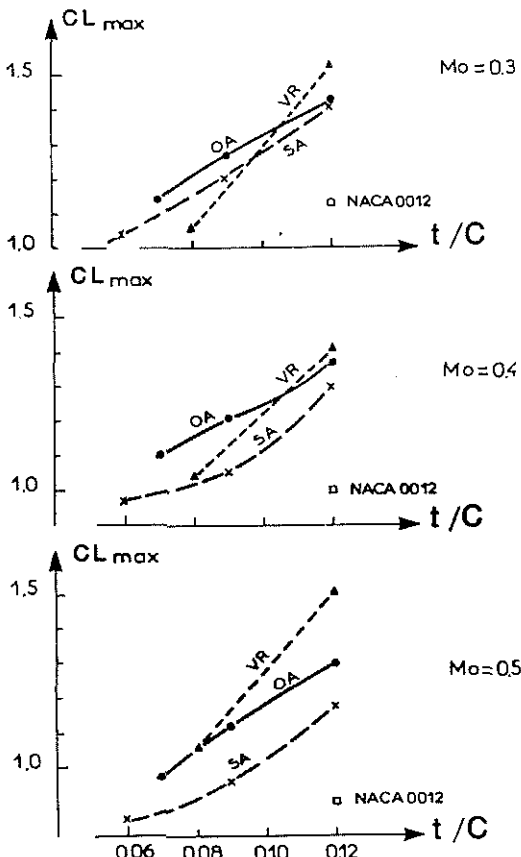


Fig. 19 Evolution of the CL max with thickness to chord ratio

Total performances of the OA family are presented versus the thickness to chord ratio on figs. 19 and 20 and compared with those of the Boeing Vertol family VRx and the Aérospatiale family SA131xx which are used on the SA330 PUMA ref. 3. Concerning the CL_{max} fig. 19 the OA family is better than the SA131xx for all the thickness to chord ratio and also better than the VRx one for the small thickness but as it has been already pointed out the VR family has good CL_{max} for $t/c = 0.12$ especially at $Mo = 0.5$. For the MDD and the Mach tuck (defined as the mach number for which $dC_{mo}/dM_o = -0.25$ in ref. 6) fig. 20 the OA family has also better performances. It is difficult to compare the L/D of the VR and OA family because the VR airfoils have not been tested in the same wind tunnel and at the same Reynolds number as the OA airfoils but nevertheless the VR8 has a low CD at $Mo = 0.6$ and $CL = 0.6$.

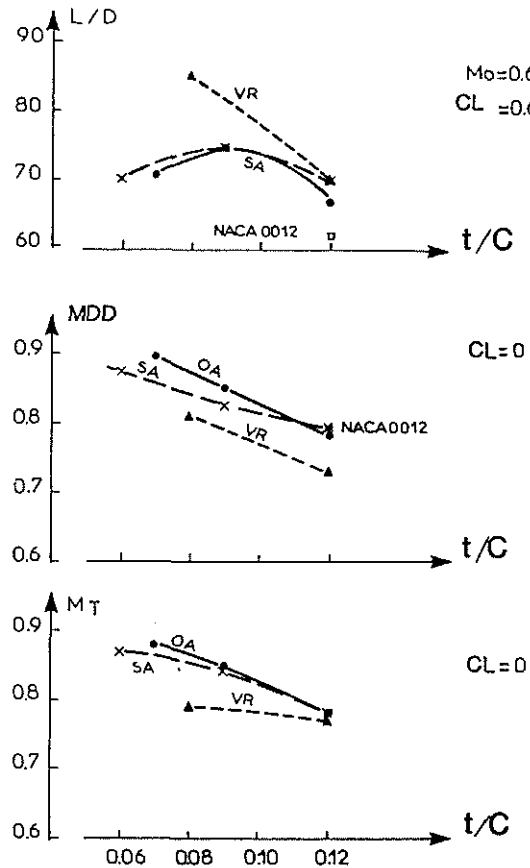


Fig. 20 Evolution of L/D, MDD and Mach tuck with thickness to chord ratio

In conclusion the overall performances of the OA family show that the main objectives (i.e. improvements in hovering and forward flight compared to classical blade) have been reached with these new airfoils.

2.5 Comparisons between theory and experiment

Figs. 21 to 24 show some comparisons between computations and experimental results on the OA207 and OA212 airfoils. Some comparisons had already been presented in ref. 4 on the OA209 airfoil. These figures show that the agreement is generally good especially for the drag polar fig. 21 and the CD evolution at constant CL fig. 22. Some discrepancies appear however in the prediction of the C_{mo} at high mach number and in the evolution of the minimum of K_p at high lift level (figs 23 and 24) due to the fact that the transonic viscous code used do not take into account the wake of the airfoil and use empirical relations to compute the boundary layer when a small separation occurs at the trailing edge.

3 - WIND TUNNEL ROTOR EXPERIMENTS

In order to test the behaviour of these new profiles on a helicopter rotor, an intensive experiment has been conducted in the large SI Modane wind tunnel (figure 25). The wind tunnel test section, 8 meters in diameter, allows testing 4 meters diameter model rotors in a conventional way, at airspeeds well beyond the speed range of the present-day helicopters (speed attained with a helicopter rotor : 132 m/s). The rotor test rig itself allows obtaining a realistic tip speed of 210 m/s.

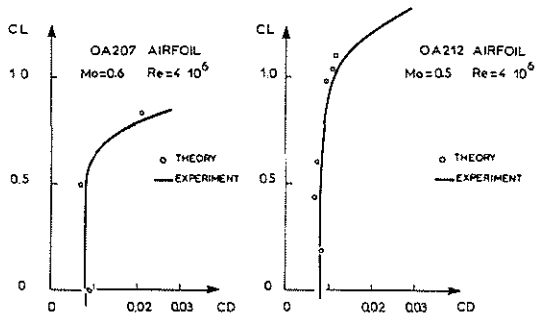


Fig. 21 Theoretical prediction of the drag polar

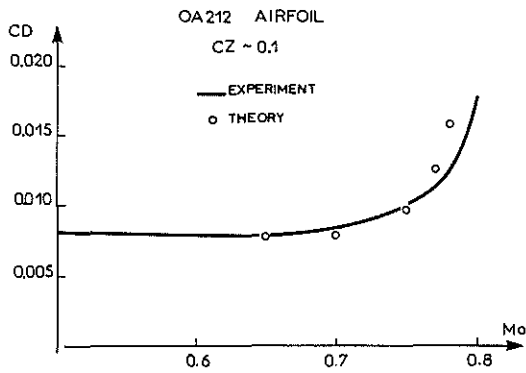


Fig. 22 Theoretical prediction of the drag evolution with Mach number

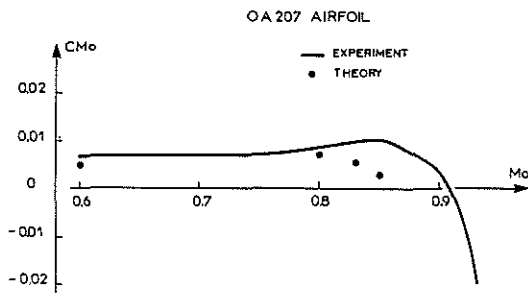


Fig. 23 Theoretical prediction of the CM_o

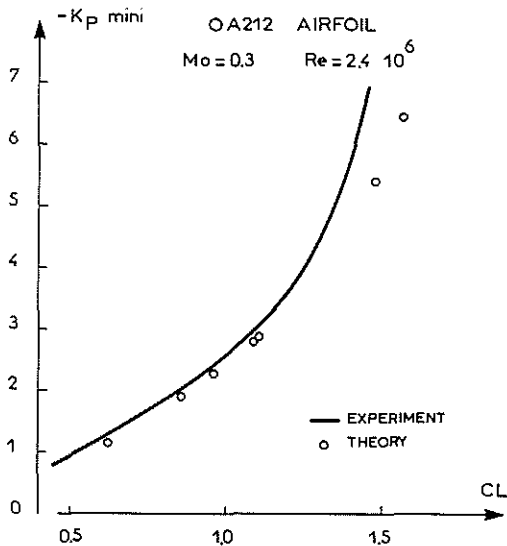


Fig. 24 Theoretical prediction of the leading edge expansion

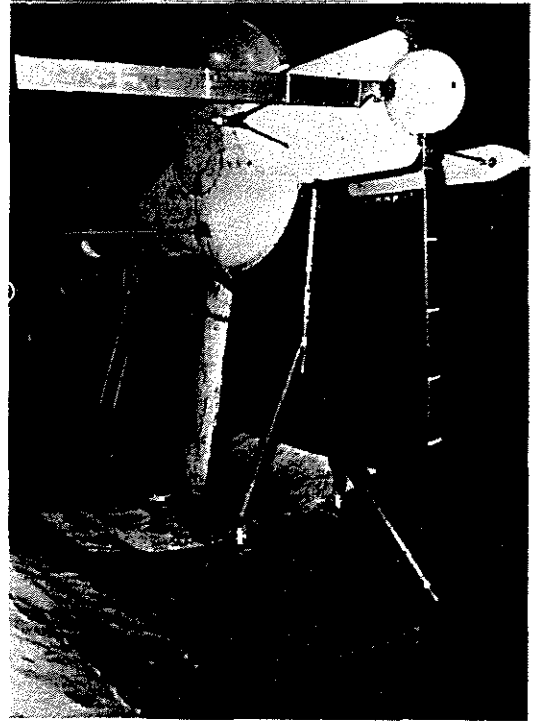


Fig. 25 SI Modane wind tunnel

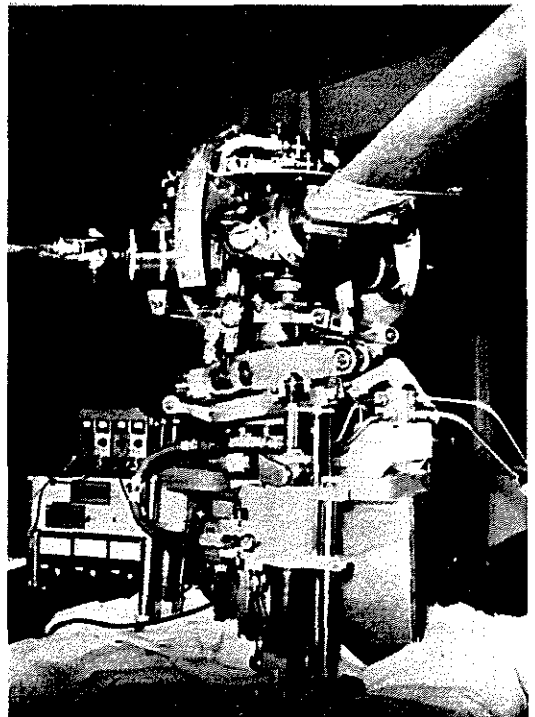


Fig. 26 Rotor hub and washplate

The rotor shaft can be tilted from + 25° to - 95° with respect to the vertical so as to cover both the forward flight (power-on and power-off) and the quasi-hover flight (rotor in axial position). The rotor test rig is equipped with a swashplate allowing the collective pitch to be changed (lift variation) and the cyclic pitch to be set for reducing the rotor blade flapping angle (figure 26) during rotation.

The technology involved in manufacturing the model rotor blades (figure 27) closely relates to that conventionally used on full size composite rotor blades. The spar is made of glass fiber roving whereas the rear section consists of a honeycomb filler. The rotor blade skin is made of 45° crossed carbon fabric layers, whose thickness decreases towards the trailing edge. A thin glass cloth layer protects the carbon skin. The trailing edge consists of a carbon trailing edge strip fitted at the junction of upper and lower surface carbon skin. Chordwise blade balance is achieved by adding an INERMET counterweight embedded in the spar.

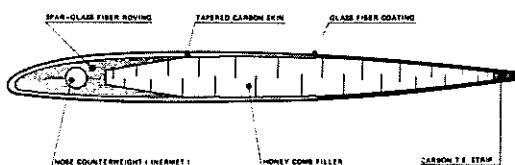


Fig. 27 Model blade technology

So, though these rotor blades are not strictly dynamically similar to full size rotor blades (LOCK number twice lower for a model rotor blade), their natural frequencies are similar of those of an actual rotor, mainly as regards the torsion (5.2Ω at model scale), which is important for studying the dynamic behaviour of new profiles (STALL FLUTTER or MACH TUCK).

The experiments were conducted on three four-bladed rotors having a 4-meters diameter, a 140 mm chord and a -8° theoretical aerodynamic twist. The characteristics of these three rotors are summarized in the following chart :

Rotor 5	NACA 0012 from 0.2 R to 0.7 R TAPERED from 0.7 R (NACA 0012) to 0.85 R (SA 13109), to 1.0R (SA 13106).
Rotor 6A	OA209, constant
Rotor 6B	OA209, constant from 0.2R to 0.8R TAPERED from 0.8R (OA209) to 1.0R (OA207)

ROTOR AERODYNAMIC DESIGN

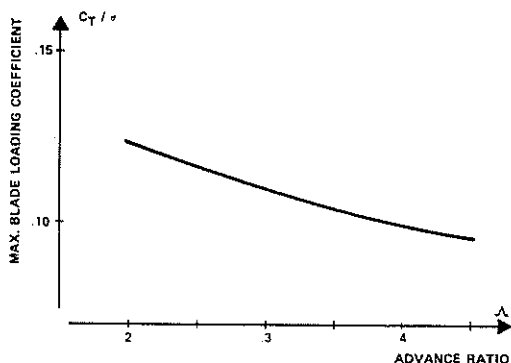


Fig. 28 Rotor test envelope

The envelope covered by these tests proved very satisfactory both in hover ($C_T/\sigma = 0.15$) and in forward flight (high rotor blade-loading : $C_T/\sigma = 0.12$; high speed : $\Lambda = 0.45$; advancing blade mach number = 0.94).

The forward flight envelope is given for information in figure 28. It should be noted that this envelope was only limited by problems of torque-meter limitations and rotor blade structural integrity and, in no case, by an abnormal behaviour of the rotors.

The results obtained in quasi-hover are better with the new profile generation (Rotors 6A and 6B) than with the reference rotor (Rotor 5) (figure 29). For low to medium loads (up to $C_T/\sigma = 0.11$), the figure of merit was improved owing to the higher lift-to-drag ratio of the OA209 airfoil section.

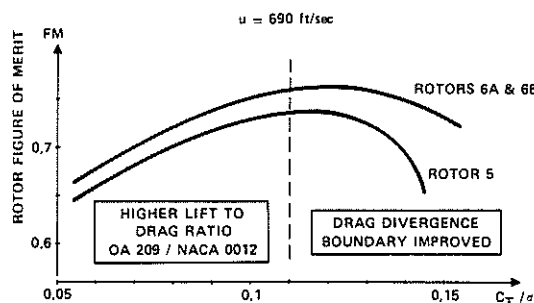


Fig. 29 Model rotor hover performance

For high loads ($C_T/\sigma > 0.11$), the improvement is still more important since OA airfoils are less sensitive to drag divergence at high load than NACA 0012 airfoils. Furthermore, tapering of rotor 6B did not induce too large sensitivity to the compressibility effect for high loads.

In forward flight (figures 30 and 31), the gain on performance is negligible within the range of medium loads and economic cruise speeds. Figure 31 shows that rotor 6B gives slightly better performance than the other two rotors. On the contrary at high speed and high load, the new generation of profiles gives a significant improvement.

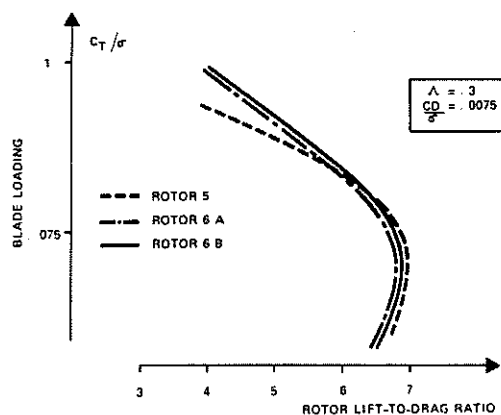


Fig. 30 Improvements on high-loaded rotor

On the one hand, the taper end section (OA207) delays the compressibility effect on the advancing blade beyond $M_{\infty} = 0.86$, which leads to a very slow evolution of the rotor profile power with the advancing blade mach number, even up to a mach number ranging about 0.93 (figure 32). Simultaneously, the dynamic behaviour of the rotors always proved fair and no Mach Tuck phenomenon has been encountered. On the other hand, the improved stall characteristics of OA airfoils enable the rotor

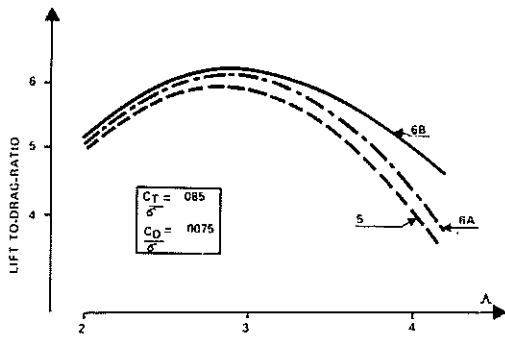


Fig. 31 Effect of advance ratio on rotor lift-to-drag ratio.

blades to operate at higher blade-loading while maintaining an adequate rotor lift-to-drag ratio (figure 30). At medium load, the small decrease in rotor lift-to-drag ratio due to the adoption of a more cambered profile, is in great part balanced by the taper end section of the OA207 airfoil. As a general rule, the behaviour of both OA airfoil rotors in stall conditions proved better as compared to that of rotor No5. The torsion oscillations generally linked with stalling in the retreating blade sector, are very quickly stabilized, at an acceptable amplitude : for information, figure 33 shows the evolution specific to the pitch change rod load versus the rotor load for rotor 6B. The sum of harmonic 5Ω et 6Ω of the signal has only been considered, since "stall flutter" phenomenon preferably excites the harmonics close to the rotor blade torsion frequency (5.2Ω).

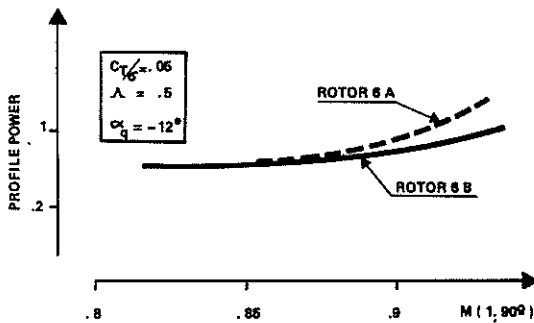


Fig. 32 Effect of compressibility on OA airfoil rotors

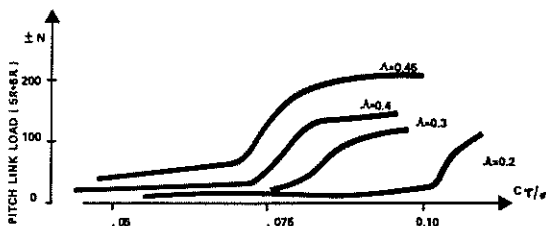


Fig. 33 Behaviour of rotor 6B in stall conditions

4 - FLIGHT TEST ROTOR EXPERIMENTS

Strictly comparative tests had enabled the better performance of OA209 airfoil in hover to be evidenced as compared to NACA 0012 airfoil ref. 4 . The first set of prototype rotor blades manufactured with a view to upgrading the Dauphin production range, confirmed the gains contemplated on hover performance. Despite slight differences in twist

($-8^\circ \rightarrow -10^\circ$) and in chord (350 mm \rightarrow 385 mm) between the reference rotor (NACA 0012) and the 3rd generation rotor (OA series), comparison between the rotor figure of merit (figure 34) brings out the improvements resulting in an increase in take-off weight of 100 kg (220 lb) approximately, for the same power.

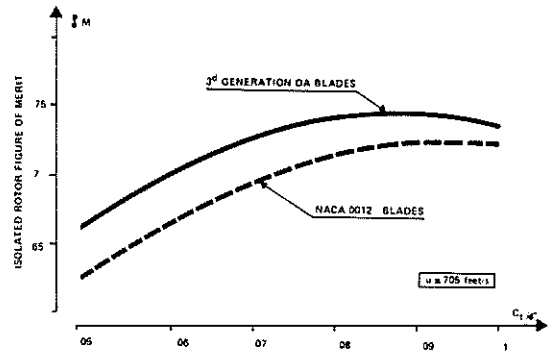


Fig. 34 Comparison of rotor efficiency from hover tests

Such an improvement also exists at low speeds, which is very important for the helicopter civil performance (engine failure case). Figure 35 shows that changing the type of rotor blade makes it possible to upgrade the take-off performance of civil aircraft by 300 kg (700 lb) approximately, considering the case where such performances are limited by the climbing law on one engine at V_y .

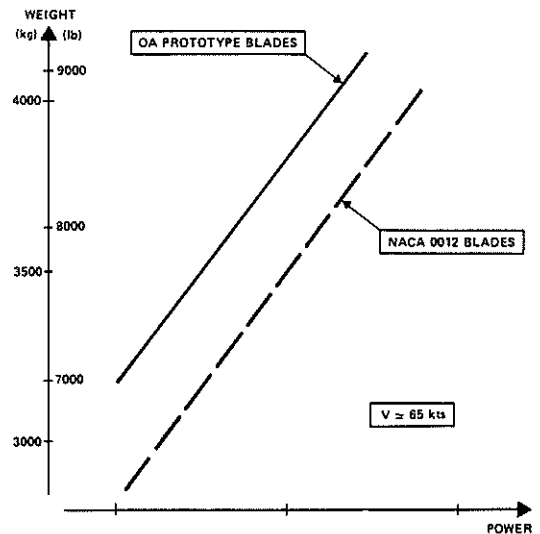


Fig. 35 Improvement on low speed performance

In forward flight, both types of rotor blades on the same Dauphin helicopter could not be fully compared especially at high speed, since fatigue substantiation at test time was not sufficiently developed. During this test campaign, the improvement noticed up to 120 knots (figure 36) seems to confirm the 3% gain expected on kilometric fuel consumption in economic cruise flight. Since these tests, the 3rd generation blades for the Dauphin have been tested on the twin-engined SA 365 C and on the 1st SA 365 N prototype. The improvement of the rotor aerodynamic efficiency has been amply confirmed, as shown fig. 37, both at the economic cruise speed and at high speed. The level flight envelope is greatly extended with this new rotor, both in speed and in weight. Fig. 38 shows clearly the DAUPHIN's increased capability in terms of maximum weight and high altitude flight. These impro-

vements are due to the new rotor design, the reduction in aircraft drag and an increase in the available power. Meanwhile, the aircraft's behaviour with a load factor is being studied and appears to be satisfactory since it can achieve $n = 2g$ at the maximum weight of 3 850 kg, a speed of 130 Kts and an altitude of approximately 1 000 m. The new rotor, combined with the Dauphin's improved drag and power levels, give this helicopter remarkably good performance [Ref. 8], which is illustrated by the speed record achieved by an Aerospatiale company aircraft on the round trip Paris-London-Paris at an average speed of 163 Kts.

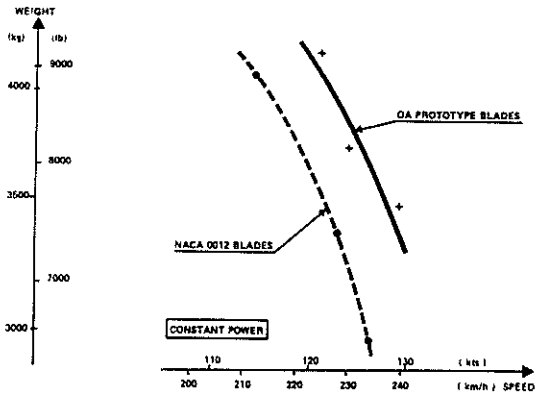


Fig. 36 Performance of OA airfoil blade in forward flight

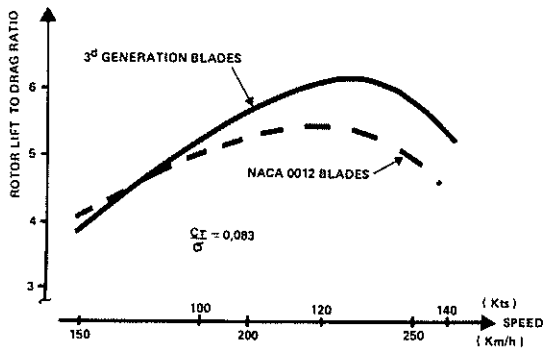


Fig. 37 Flight test comparison between OA209 and NACA 0012 airfoil rotor lift-to-drag ratio

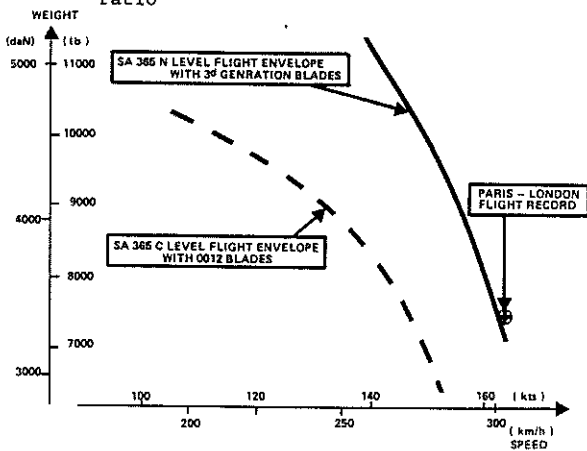


Fig. 38 Flight envelope extension with the 3rd generation blades

5 - CONCLUSIONS

1) New airfoils have been defined with maximum lift and drag divergence characteristics better than the conventional ones.

2) Most of the two dimensional characteristics of airfoils can be estimated using transonic viscous codes but maximum lift evaluation can be assessed only by separated flow analysis methods.

3) The gains in performances expected with this new generation of profiles have been experimentally checked on rotor. Results are :

- . improved figure of merit in hovering flight.
- . better lift to drag ratio at high speed and under heavy load.

4) These significant results made it possible to provide the Dauphin helicopters with a new rotor permitting :

- . an increase in gross weight
- . an upgrading of military and civil take-off weights
- . an increase in maximum speed
- . a higher manoeuvrability

5) The effort in research must still be sustained in order to improve the rotor performance at high speed and under load factors.

REFERENCES

- 1 G. Petit - The helicopters and energy savings, paper presented at the 13th International Congress for Aeronautics, Paris June 2 and 3 1977.
- 2 M. Lecarme - Rotor behaviour beyond normal operating conditions at the large S1 Modane-Avrieux wind tunnel facilities AGARD CP-111, 1973.
- 3 J. Renaud and F. Nibelle - Effects of the airfoil choice on rotor aerodynamic behaviour in forward flight. Paper presented at the 2nd European Rotorcraft and Powered Lift Aircraft Forum Bückeburg September 1976.
- 4 J.J. Thibert and J. Gallot - A new family for rotor blades, Paper presented at 3th European Rotorcraft and powered Lift Aircraft Forum, 1977.
- 5 J. Bousquet - Calculs bidimensionnels transoniques avec couche limite 11ème Colloque AAAF 1974.
- 6 Leo Dadone - Rotor airfoil optimization : an understanding of the physical limits, paper presented at 34th Annual National AHS Forum May 1978.
- 7 US Army helicopter design datcom Volume I, Airfoils Boeing Doc N° 0210-1197-1 May 1976.
- 8 P. Roesch, Aerodynamic design of the Aerospatiale AS 365 N Dauphin 2 helicopter, paper presented at 6th European Rotorcraft and Powered Lift Aircraft Forum, 1980.